hv photonics

IMPACT FACTOR 2.4

CITESCORE 2.3

Article

One-Step Implementation of Collective Anti-Blockade in a Rydberg Ring

Yijiao Fu and Jinhui Wu

MDPI

https://doi.org/10.3390/photonics10101172

photonics

MDPI

Article

One-Step Implementation of Collective Anti-Blockade in a Rydberg Ring

Yijiao Fu and Jinhui Wu *

Center for Quantum Sciences and School of Physics, Northeast Normal University, Changchun 130024, China; fuyj593@nenu.edu.cn

* Correspondence: jhwu@nenu.edu.cn

Abstract: In contrast to Rydberg blockade, Rydberg anti-blockade allows multiple atoms to be simultaneously excited in the presence of significant nonlocal interactions and can lead to distinct phenomena and applications. This inspires us to examine here general conditions, numerical verifications, and realistic restrictions regarding the collective anti-blockade excitations of N Rydberg atoms equally arranged along a ring. We find that by adjusting the detuning of a pump field to compensate for nonlocal interactions between one atom and all others, it is viable to realize resonant excitations of N atoms but suppress far-detuned excitations of $N-1$ and fewer atoms under different conditions for an odd and an even number of atoms. Population dynamics of this Rydberg ring further show that one-step anti-blockade implementation can be attained at a cutoff time of the pump field, which increases quickly with the number of atoms. Hence, roughly perfect anti-blockade excitations are attainable only for a not-too-large N due to inevitable spontaneous Rydberg decay.

Keywords: Rydberg atoms; Rydberg anti-blockade; population dynamics

check for updates

Citation: Fu, Y.; Wu, J. One-Step Implementation of Collective Anti-Blockade in a Rydberg Ring. *Photonics* **2023**, *10*, 1172. https://doi.org/10.3390/photonics10101172

Received: 27 September 2023
Revised: 17 October 2023
Accepted: 19 October 2023
Published: 20 October 2023

1. Introduction

Highly excited Rydberg atoms of principal quantum numbers $n \gg 1$ are a promising neutral-atom platform for realizing quantum computing, simulation, metrology, and so on [1] due to their nontrivial features, including large dipole moments, long radiative lifetimes, and strong nonlocal interactions [2]. It is of particular interest that nonlocal Rydberg interactions, usually manifested as van der Waals (vdW) interactions ($\propto n^{11}/r_{ij}^6$) or dipole–dipole interactions ($\propto n^4/r_{ij}^3$) with r_{ij} being the distance between two atoms i and j, may prohibit the same Rydberg excitations of other atoms within a mesoscopic volume by inducing a large enough energy shift when one atom has been excited to a Rydberg state by a resonant pump field. This is the so-called Rydberg blockade effect [3,4], an effective resource for implementing multi-qubit gates [5,6], spatial Kramers–Kronig relations [7], electromagnetically-induced grating [8,9], multi-particle entanglement [10–12], single-photon sources [13,14], etc.

An opposite effect is Rydberg anti-blockade [15], which allows the simultaneous excitations of multiple atoms to a common Rydberg state. It was first proposed in [16] and subsequently realized in [17] by considering a three-level ladder system of ultracold Rydberg gas. So far, two methods of Rydberg anti-blockade have been proposed: one is the simultaneous driving [18,19] where a coherent field is suitably detuned to compensate for the (average) Rydberg shift so as to realize collective excitations of all atoms from the ground state to the Rydberg state; another is the sequential driving [20] where a first coherent field resonantly excites one atom to a Rydberg state while a second coherent field excites other atoms to the same state by compensating for the (average) Rydberg shift with a suitable detuning. There have been extensive studies on the realization and application of the Rydberg anti-blockade for atomic pairs or ensembles [21–31], while little attention has been paid to regularly arranged finite atoms, e.g., in a ring or a square optical lattice.

With the development of state-of-the-art techniques, it is now viable to precisely capture and arrange a finite number of cold atoms using optical tweezers. We note, in particular, that Lukin et al. have prepared one-dimensional atomic arrays [32] while two-dimensional [33,34] and three-dimensional atomic arrays [35] have been implemented using the technology of mobile optical tweezers. Recently, it has been shown that defect-free large-scale and heterogeneous atomic arrays could also be realized in experiments [36]. These regular atomic structures have been explored for different purposes, e.g., to implement quantum logic gates based on atomic qubits [37–41] and quantum simulation tasks such as Ising-like [42–44] and XY-spin Hamiltonians [45–47]. As far as we know, they are rarely studied for achieving Rydberg anti-blockade and relevant applications.

In this work, we consider a two-dimensional ring model of two-level Rydberg atoms illuminated by a pump laser to realize their collective anti-blockade in one step. First, we aim at deriving the general anti-blockade conditions with respect to an odd and an even number of equally separated Rydberg atoms, respectively. Then, we try to attain the pump field cutoff time when all atoms are excited from the ground state to the Rydberg state yet without populating all intermediate states. Finally, we examine the population dynamics of three-, four-, five-, and six-atom systems via numerical simulations to verify analytical expectations on one hand and find realistic restrictions on the other hand. It is found that the perfect elimination of all intermediate states requires a large enough ratio between the pump detuning and Rabi frequency. This inevitably results in a cutoff time increasing quickly with the number of atoms so that spontaneous Rydberg decay, though typically very small, is negligible just for a few atoms. Hence, the strategy of using a pump laser to achieve one-step Rydberg anti-blockade is valid only for a not-too-large number of atoms.

2. Model and Equations

2.1. Level Configuration and Geometric Arrangement

We consider in Figure 1 a few identical two-level atoms with the ground $|g\rangle$ and Rydberg $|r\rangle$ states loaded into optical traps of equal distance r_{n1}, typically in the range of $\{2, 10\}$ μm [42,48,49]. They are driven by a common pump field of frequency ω_p and amplitude E_p with detuning $\Delta_p = \omega_p - \omega_{rg}$ and Rabi frequency $\Omega_p = E_p\mu_{gr}/2\hbar$, where ω_{rg} and μ_{gr} have been defined as resonant frequency and dipole moment on transition $|g\rangle \leftrightarrow |r\rangle$, respectively. Any two of the N trapped atoms interact also through a van der Waals (vdW) potential $V_{ij} = C_6/r_{ij}^6$ with C_6 being the vdW coefficient and r_{ij} the distance between atom i and atom j. This consideration is valid when r_{n1} is large enough to exceed the vdW distance d_{vdW} for a certain Rydberg state, which can be estimated with the ARC Toolkit [50]. In our ring model, the atoms can be fixed either by tight optical tweezers [32–36] or in deep optical lattices [51–53], leaving atomic position fluctuations negligible as compared to r_{n1} for ultracold atoms, e.g., at the sub μK temperatures.

In the interaction picture, with the rotating-wave and electric-dipole approximations, the total Hamiltonian of an N-atom system is $\mathcal{H}_N = \mathcal{H}_a + \mathcal{H}_v$, where

$$\mathcal{H}_a = \hbar \sum_{i=1}^{N} [-\Delta_p |r\rangle_i\langle r| + (\Omega_p |r\rangle_i\langle g| + H.c.)], \tag{1}$$

denotes the atom–field interactions while

$$\mathcal{H}_v = \hbar \sum_{i=1}^{N-1} \sum_{j=i+1}^{N} V_{ij} |rr\rangle_{ij}\langle rr|, \tag{2}$$

denotes the atom–atom interactions. In order to facilitate discussions, we separately deal with two specific cases where an even or an odd number of Rydberg atoms are equally arranged along a ring. We will examine, in particular, with Hamiltonian $\mathcal{H}_N$, the general conditions for realizing an anti-blockade effect as well as their numerical verifications and realistic restrictions for the even-number and odd-number cases, respectively.

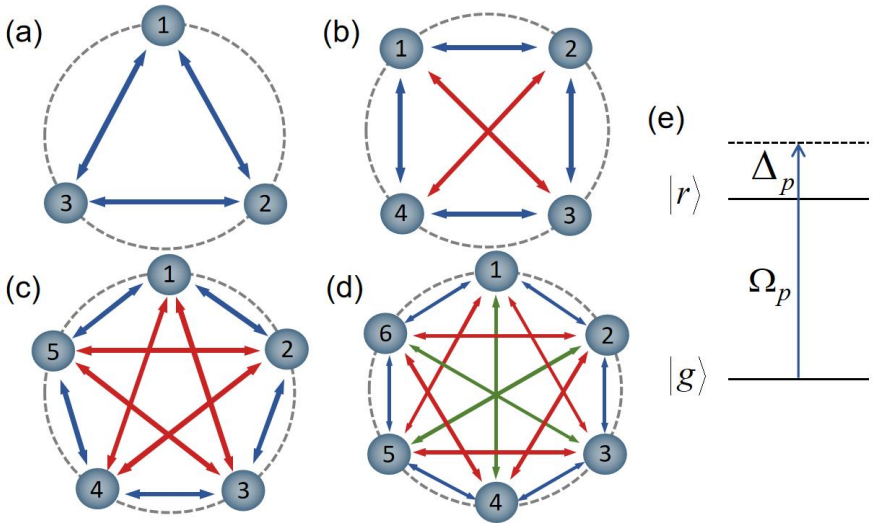

Figure 1. Geometric arrangements for (**a**) three, (**b**) four, (**c**) five, and (**d**) six Rydberg atoms equally spaced along a ring. Blue, red, and green lines with arrows represent nearest, next-nearest, and next-next-nearest neighbor interactions between different atomic pairs, respectively. (**e**) Two-level configuration for each atom arranged along the ring when a coherent pump field is applied to couple ground state $|g\rangle$ to Rydberg state $|r\rangle$ with Rabi frequency Ω_p and detuning Δ_p.

2.2. Anti-Blockade Conditions of Rydberg Excitations

2.2.1. A Ring of Odd-Number Rydberg Atoms

Here we start from the simplest three-atom case (see Figure 1a) to derive a corresponding anti-blockade condition with the energy level diagram given in Figure 2. In this case, the interactions of all Rydberg pairs are identical with $V_{12} = V_{23} = V_{13} = V_1$ since any two atoms are equally spaced along the ring. Then, if ground state $|ggg\rangle$ is assumed to exhibit a zero energy, as usual, the energies of singly excited states $|ggr\rangle$, $|grg\rangle$, and $|rgg\rangle$ will remain unshifted with $E = \hbar\omega_{rg}$ in the absence of any Rydberg interactions; the energies of doubly excited states $|grr\rangle$, $|rrg\rangle$, and $|rgr\rangle$ will be shifted from $2E$ to $2E + \hbar V_1 = 2\hbar\omega_{rg} + \hbar V_1$ due to a single Rydberg interaction; the energy of fully excited state $|rrr\rangle$ will suffer a larger shift from $3E$ to $3E + 3\hbar V_1 = 3\hbar\omega_{rg} + 3\hbar V_1$ in the presence of three pairs of Rydberg interactions.

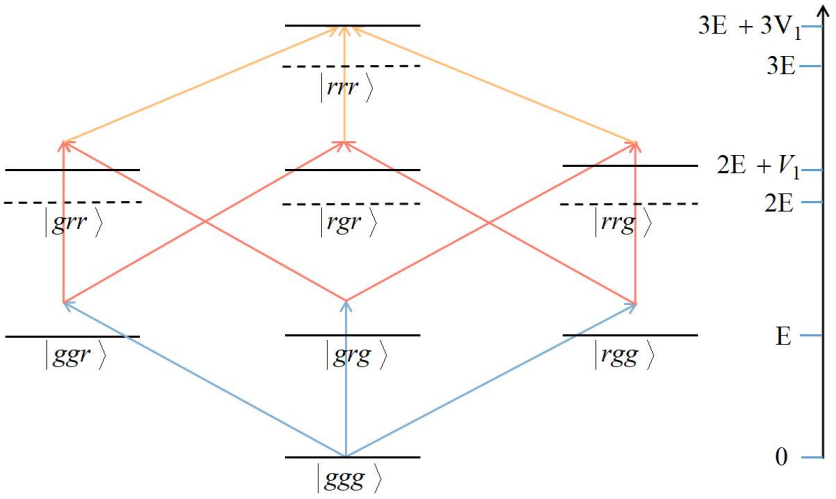

Figure 2. Eight-level configuration in the three-atom basis, where singly, doubly, and fully excited Rydberg states exhibit different shifts due to vanishing or nonzero *vdW* interactions. The pump field is applied on three-photon resonance yet with large single-photon and two-photon detunings.

One key to realizing the collective anti-blockade effect is to compensate the energy shift of fully excited state $|rrr\rangle$ caused by Rydberg interactions with an appropri-

ate detuning of the coherent pump field. In other words, we should try to attain the resonant excitation between $|ggg\rangle$ and $|rrr\rangle$ by modulating the coherent pump field to achieve $3\hbar\omega_p = 3E + 3\hbar\Delta_p = 3E + 3\hbar V_1$, i.e., $\Delta_p = V_1$. Note, however, that we also need to avoid populating all intermediate (singly and doubly) excited states by making them far-detuned from the ground state. More specifically, in the case of $\Delta_p = V_1$, the single-photon detuning $(E + \hbar\Delta_p) - E = \hbar V_1$ is identical to the two-photon detuning $(2E + 2\hbar\Delta_p) - (2E + \hbar V) = \hbar V_1$. Then, the three-atom anti-blockade condition should be

$$\Delta_p = V_1 \gg \Omega_p, \tag{3}$$

so as to suppress the excitation of all (singly and doubly excited) intermediate states.

In the five-atom case, however, there are two kinds of Rydberg interactions (see Figure 1c) in the presence of two groups of atomic pairs with different spacings. Hence, we should define $V_{12} = V_{23} = V_{34} = V_{45} = V_{15} = V_1$ as the nearest neighbor interactions and $V_{13} = V_{14} = V_{24} = V_{25} = V_{35} = V_2$ as the next-nearest neighbor interactions. Via a similar analysis, it is not difficult to attain the five-atom anti-blockade condition

$$\Delta_p = V_1 + V_2 \gg \Omega_p, \tag{4}$$

required for realizing the resonant excitation of the fully excited state $|rrrrr\rangle$ and meanwhile suppressing the far-detuned excitations of all intermediate states.

Through careful induction, the general anti-blockade condition for $N = 2k + 1$ $(k = 1, 2, 3, \dots)$ equally spaced atoms along a ring can be summarized as

$$\Delta_p = \sum_{i=1}^{k} C_6 \left(\frac{\sin\frac{\alpha}{2}}{r_{n1} \sin i\frac{\alpha}{2}} \right)^6 \gg \Omega_p, \tag{5}$$

where the *vdW* potentials V_i have been expressed as a function of coefficient C_6, distance r_{n1}, index i, and angle $\alpha = 2\pi/N$ (see Appendix A for details).

2.2.2. A Ring of Even-Number Rydberg Atoms

Here we start from the four-atom case (see Figure 1b) since the simplest two-atom case has been well discussed in previous works [10,20,25,27,39] with the anti-blockade condition being simply $\Delta_p = 0.5V_1 \gg \Omega_p$. In this four-atom case, there exist both nearest (V_1) and next-nearest (V_2) neighbor interactions, which exhibit different contributions to the shift of an excited state containing two or more Rydberg atoms as can be found in the energy level diagram given in Figure 3.

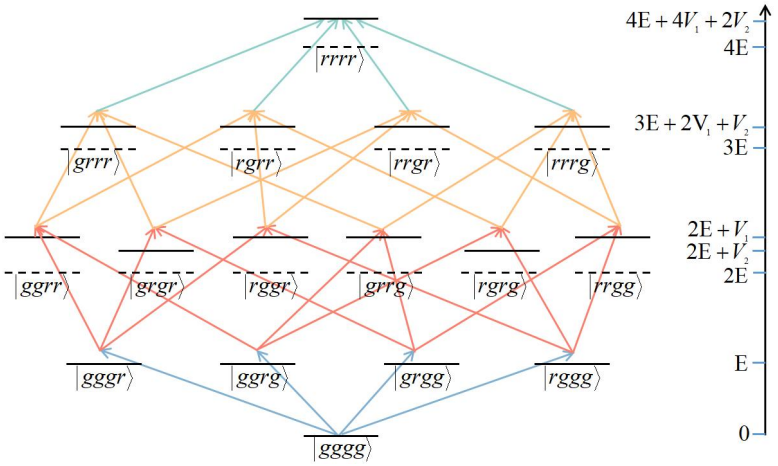

Figure 3. Sixteen-level configuration in the four-atom basis, where singly, doubly, triply, and fully excited Rydberg states exhibit different shifts due to different *vdW* interactions. The pump field is applied on four-photon resonance with large one, two, and three-photon detunings.

In the spirit of relevant discussions on three-atom anti-blockade, four-photon resonance is required to realize a full transfer of all atoms from ground state $|g\rangle$ to Rydberg state $|r\rangle$, i.e., $4\hbar\omega_{rg} = 4E + 4\hbar\Delta_p = 4E + 4\hbar V_1 + 2\hbar V_2$, thus yielding $\Delta_p = V_1 + 0.5V_2$. In this case, it is not difficult to find that both single-photon and three-photon detunings are $V_1 + 0.5V_2$ while the two-photon detuning is $V_1 + V_2$ or $2V_1$. Considering that $2V_1 > V_1 + V_2 > V_1 + 0.5V_2$ due to $V_1 > V_2$, it is viable to avoid populating all intermediate (singly, doubly, and triply) excited states with sufficiently large pump detunings

$$\Delta_p = V_1 + 0.5V_2 \gg \Omega_p, \tag{6}$$

for realizing a four-atom anti-blockade.

As to the six-atom case, a similar analysis allows us to find the following anti-blockade condition

$$\Delta_p = V_1 + V_2 + 0.5V_3 \gg \Omega_p, \tag{7}$$

with V_3 denoting the next-next-nearest neighbor interactions. Via careful induction, the general anti-blockade condition for $N = 2k$ ($k = 1, 2, 3, 4, \ldots$) equally spaced atoms along a ring can be summarized as

$$\Delta_p = \frac{C_6}{2}\left(\frac{\sin\frac{\alpha}{2}}{r_{n1}}\right)^6 + \sum_{i=1}^{k-1} C_6\left(\frac{\sin\frac{\alpha}{2}}{r_{n1}\sin i\frac{\alpha}{2}}\right)^6 \gg \Omega_p, \tag{8}$$

clearly different from Equation (5) for an odd number of Rydberg atoms (see Appendix A for details).

2.3. Effective Hamiltonians and Cutoff Times

In realistic experiments, a perfect transfer of all atoms from ground state $|g\rangle$ to Rydberg state $|r\rangle$ could be attained only if the pump field is cut off at an appropriate time. To this end, we first choose the three-atom system as an example to calculate its effective Hamiltonian [54] when all intermediate states are safely eliminated under the anti-blockade condition $\Delta_p = V_1 \gg \Omega_p$. With details on the calculation procedure given in Appendix B, we can write down the effective Hamiltonian

$$\mathcal{H}_3^{\mathtt{eff}} = \hbar\delta_3^{\mathtt{eff}}(|ggg\rangle\langle ggg| + |rrr\rangle\langle rrr|) + (\hbar\Omega_3^{\mathtt{eff}}|ggg\rangle\langle rrr| + H.c.), \tag{9}$$

where $\Omega_3^{\mathtt{eff}} = 6\Omega_p^3/\Delta_p^2$ represents the effective pump Rabi frequency while $\delta_3^{\mathtt{eff}} = 3\Omega_p^2/\Delta_p$ is the common Stark shift of both ground state $|ggg\rangle$ and fully excited state $|rrr\rangle$. This shift arising from the virtual absorption and emission of pump photons is trivial and can be removed in calculations because, as two identical diagonal terms, they will not result in a three-photon detuning; hence, they do not participate in the anti-blockade dynamic evolution.

To be more specific, we assume that the effective pump field is a squared pulse of duration τ_3 and the three atoms are initially prepared in ground state $|ggg\rangle$. Then, the anti-blockade cutoff time, i.e., τ_3 for a $\pi/2$ squared pump pulse, can be calculated through

$$|\Omega_3^{\mathtt{eff}}|\tau_3 = \frac{\pi}{2}, \tag{10}$$

at which the three atoms will be in a fully excited state $|rrr\rangle$ as verified in the next section.

Effective Hamiltonians $\mathcal{H}_4^{\mathtt{eff}}$, $\mathcal{H}_5^{\mathtt{eff}}$, and $\mathcal{H}_6^{\mathtt{eff}}$ for four-atom, five-atom, and six-atom systems, respectively, are listed in Appendix B with which it is easy to learn the corresponding effective pump Rabi frequencies $\Omega_4^{\mathtt{eff}}$, $\Omega_5^{\mathtt{eff}}$, and $\Omega_6^{\mathtt{eff}}$. Then, the cutoff times τ_4, τ_5, and τ_6 can be calculated via $|\Omega_N^{\mathtt{eff}}|\tau_N = \pi/2$.

3. Results and Discussion

In this section, we examine the dynamic evolutions of a few N-atom systems under the anti-blockade conditions attained above. This will be conducted by numerically solving the master equation of density operator ρ

$$\partial_t \rho = -i/\hbar[\mathcal{H}_N, \rho] + \mathcal{L}(\rho), \tag{11}$$

where $\mathcal{L}(\rho) = \frac{1}{2}\sum_{j=1}^{N}[2\mathcal{L}_j\rho\mathcal{L}_j^\dagger - \mathcal{L}_j^\dagger\mathcal{L}_j\rho - \rho\mathcal{L}_j^\dagger\mathcal{L}_j]$ is the Lindblad operator describing the dissipation process with $\mathcal{L}_j = \sqrt{\Gamma}|g\rangle_j\langle r|$. Here, Γ represents the spontaneous decay rate and $|g\rangle_j\langle r|$ represents the lowering operator for atom j. Approximate numerical results can also be attained by replacing $\mathcal{H}_N$ with $\mathcal{H}_N^{\mathtt{eff}}$ to consider only the ground state and the fully excited state.

First, we plot in Figure 4 the population dynamic evolutions in the ground and the fully excited states for three atoms equally spaced along a ring in the absence (a) or presence (b) of spontaneous Rydberg decay. Figure 4a shows that the dashed lines attained with the effective Hamiltonian $\mathcal{H}_3^{\mathtt{eff}}$ and the solid lines attained with the original Hamiltonian $\mathcal{H}_3$ overlap well, indicating that all intermediate states can be safely eliminated since populations evolve only between the ground and fully excited states. Note, in particular, that the vertical dotted line refers to the cutoff time $\tau_3 \simeq 1.78$ μs where we have $\rho_{rr,rr,rr} \to 1$, indicating that a roughly perfect anti-blockade Rydberg excitation can be achieved in one step. Figure 4b further shows that a rather ideal anti-blockade Rydberg excitation $\rho_{rr,rr,rr} > 0.99$ can be attained even in a more realistic situation with $\Gamma = 2\pi \times 1\,\mathrm{ms}^{-1}$, which just results in a small number of populations leaked out to the intermediate states in a limited time $t = \tau_3$.

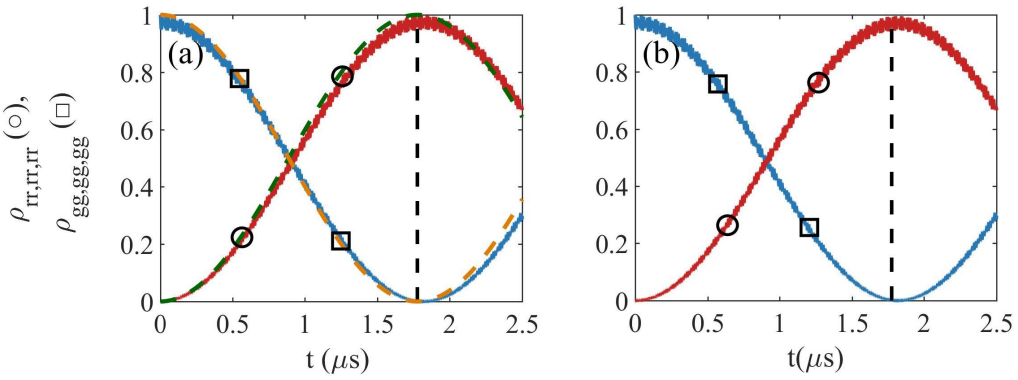

Figure 4. Population evolutions of ground (squares) and fully excited (circles) states for the three-atom system with (**a**) $\Gamma = 0$; (**b**) $\Gamma = 2\pi \times 1\,\mathrm{ms}^{-1}$ [55]. Solid lines refer to exact results attained with $\mathcal{H}_3$, while dashed lines refer to approximate results attained with $\mathcal{H}_3^{\mathtt{eff}}$. Vertical dotted lines denote the cutoff time τ_3. Other parameters are $\Delta_p = V_1 \simeq 500$ MHz, $\Omega_p = \Delta_p/15$, and $\rho_{gg,gg,gg}(0) = 1.0$ with $r_{n1} \simeq 2.56$ μm and $C_6 = 140$ GHz μm^{-6} for state $|r\rangle = |60S\rangle$ of ^{87}Rb atoms.

Then, we examine in Figure 5, how the anti-blockade condition $\Delta_p = V_1 \gg \Omega_p$ depends on the ratio Δ_p/Ω_p and how the cutoff time τ_3 varies against the ratio Δ_p/Ω_p for a fixed Ω_p in the more realistic situation with $\Gamma = 2\pi \times 1\,\mathrm{ms}^{-1}$. Figure 5a shows that a population in the fully excited state is already quite large with $\rho_{rr,rr,rr} > 0.92$ at $\Delta_p/\Omega_p \simeq 10$ but gradually achieves a maximal value $\rho_{rr,rr,rr} > 0.99$ at $\Delta_p/\Omega_p \simeq 15$, indicating a roughly perfect population transfer from state $|ggg\rangle$ to state $|rrr\rangle$. With the further increase in Δ_p/Ω_p, however, it seems that $\rho_{rr,rr,rr}$ decreases a little bit, which can be attributed to the more accumulated spontaneous decay at a longer cutoff time since $\rho_{rr,rr,rr}$ becomes saturated for $\Delta_p/\Omega_p \gtrsim 15$ if we set $\Gamma = 0$. This is verified by Figure 5b where the cutoff time slowly prolongs from $\tau_3 \simeq 0.5$ μs at $\Delta_p/\Omega_p = 10$, to $\tau_3 \simeq 1.8$ μs at $\Delta_p/\Omega_p = 15$, $\tau_3 \simeq 4.2$ μs at $\Delta_p/\Omega_p = 20$, and $\tau_3 \simeq 8.2$ μs at $\Delta_p/\Omega_p = 25$.

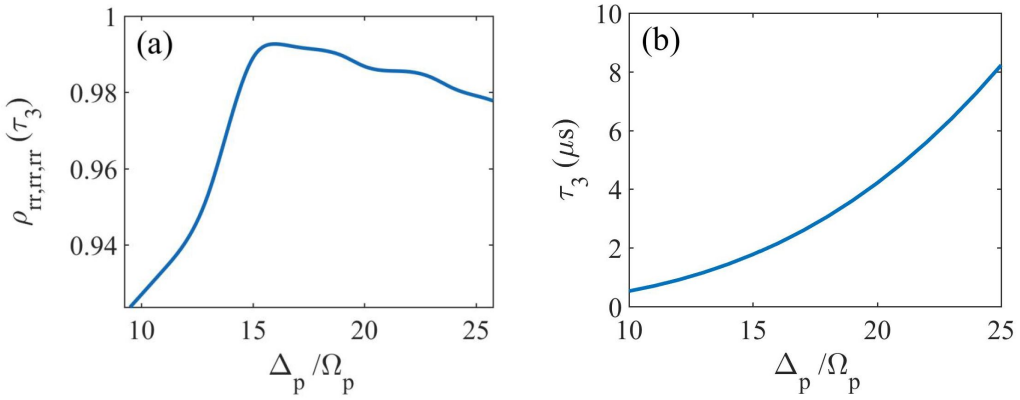

Figure 5. (**a**) Population of the fully excited state at the cutoff time and (**b**) the cutoff time against the scaled pump detuning Δ_p/Ω_p with $\Omega_p = 33$ MHz for the three-atom system. Other parameters are the same as in Figure 4.

Now, we transfer to the case where more atoms are arranged along a ring and consider in Figure 6 the four-atom, five-atom, and six-atom systems as an example. From the left three panels (a, c, e) we can see that, in the absence of spontaneous Rydberg decay, the deviation of approximate results attained with $\mathcal{H}_N^{\mathtt{eff}}$ from exact results attained with $\mathcal{H}_N$ becomes more and more evident with the increase in the number N of atoms, but it is still acceptable for $N = 6$ with the approximate and exact maximal values being $\rho_{rr,rr,rr,rr,rr,rr} \simeq 0.97$ and $\rho_{rr,rr,rr,rr,rr,rr} \simeq 0.99$, respectively, at the cutoff time $\tau_6 \simeq 146.1$ μs. This once again confirms the validity of our effective Hamiltonian method by eliminating all intermediate states, hence the validity of our one-step anti-blockade strategy from the ground state to the fully excited state. Note that the cutoff time τ_N increases quickly with number N of atoms and we have $\tau_4 \simeq 7.8$ μs, $\tau_5 \simeq 34.3$ μs, $\tau_6 \simeq 146.1$ μs, in particular, because a direct transition between the ground state and the fully excited state requires an N-photon process with the effective Rabi frequency $\Omega_N^{\mathtt{eff}}$ exactly or roughly proportional to $\Omega_p(\Omega_p/\Delta_p)^{N-1}$. Hence, $\Omega_N^{\mathtt{eff}}$ decreases rapidly with N for fixed values Ω_p and $\Omega_p/\Delta_p \ll 1$. The right three panels (b,d,f) show instead the exact results attained in the presence of spontaneous Rydberg decay, from which we find that the cutoff time τ_N becomes evidently less on one hand and the maximal value $\rho_{rr,\ldots,rr}$ largely reduces on the other hand.

To gain a clearer picture of the observations in Figure 6, we finally examine in Figure 7 how the fully excited state is populated at the cutoff time for different numbers of atoms. Figure 7a shows that τ_N increased quickly with N and reached about 146 μs for $\Gamma = 0$ while 140 μs for $\Gamma = 2\pi \times 1\,\mathrm{ms}^{-1}$ in the case of $N = 6$ as other parameters remained fixed. The quick increase in τ_N with N then resulted in what is observed in Figure 7b: $\rho_{rr,\ldots,rr}(\tau_N)$ depends weakly on N in the absence of spontaneous Rydberg decay but is sensitive to N in the presence of spontaneous Rydberg decay. To be more specific, we have $\rho_{rr,rr,rr,rr,rr,rr}(\tau_6) \simeq 0.97$ for $\Gamma = 0$ while $\rho_{rr,rr,rr,rr,rr,rr}(\tau_6) \simeq 0.64$ for $\Gamma = 2\pi \times 1\,\mathrm{ms}^{-1}$. It is also clear that a better anti-blockade effect can be realized for a shorter cutoff time. Hence, we have made similar calculations in Figure 7c,d by replacing $\Delta_p/\Omega_p = 15$ with $\Delta_p/\Omega_p = 12$, which still works for eliminating the intermediate states. It is found that the cutoff time has been largely reduced (e.g., with $\tau_6 \simeq 38$ μs) and the fully excited state becomes more populated (e.g., with $\rho_{rr,rr,rr,rr,rr,rr}(\tau_6) \simeq 0.85$). Note, in particular, that a rather good anti-blockade effect can be attained for $N = 5$ and $\Gamma = 2\pi \times 1\,\mathrm{ms}^{-1}$, as characterized by $\rho_{rr,rr,rr,rr,rr}(\tau_5) \simeq 0.93$ at $\tau_5 \simeq 11$ μs.

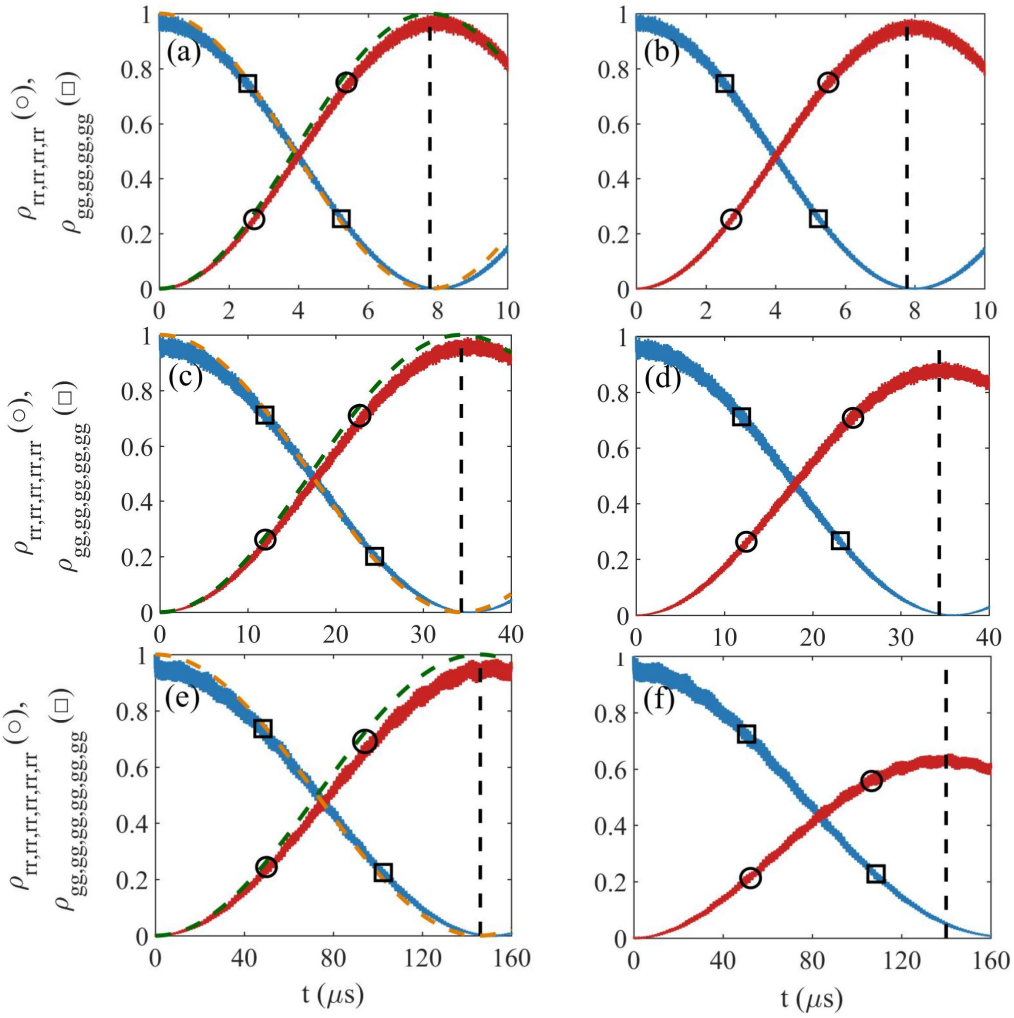

Figure 6. Dynamic evolutions of ground (squares) and fully excited (circles) states for the (**a**,**b**) four-atom, (**c**,**d**) five-atom, and (**e**,**f**) six-atom systems with (**a**,**c**,**e**) $\Gamma = 0$; (**b**,**d**,**f**) $\Gamma = 2\pi \times 1\,\mathrm{ms}^{-1}$. Solid lines refer to exact results attained with $\mathcal{H}_{4,5,6}$, while dashed lines refer to approximate results attained with $\mathcal{H}^{\mathtt{eff}}_{4,5,6}$. Vertical dotted lines denote the cutoff time τ_N. Other parameters are the same as in Figure 4.

Finally, we examine in Figure 8 how fast population $\rho_{rr,\ldots,rr}(\tau_N)$ in the fully excited state decays as Γ gradually increases for different atomic systems. It is clear that a faster Rydberg population decay occurs always for a larger number N of atoms in a ring of dipole traps and/or a larger ratio Δ_p/Ω_p between the probe detuning and Rabi frequency. Note, in particular, that the Rydberg population decay is negligible for $N = 3$ and $N = 4$, turns out to be visible for $N = 5$, but becomes remarkable for $N = 6$ in the case of $\Gamma < 1$ kHz. To be more specific, we have $\rho_{rr,rr,rr,rr,rr,rr}(\tau_6) = 0.97$ for $\Gamma = 0$ while $\rho_{rr,rr,rr,rr,rr,rr}(\tau_6) = 0.64$ for $\Gamma = 2\pi \times 1\,\mathrm{ms}^{-1}$ in Figure 8a with $\Delta_p/\Omega_p = 15$; $\rho_{rr,rr,rr,rr,rr,rr}(\tau_6) = 0.95$ for $\Gamma = 0$ while $\rho_{rr,rr,rr,rr,rr,rr}(\tau_6) = 0.85$ for $\Gamma = 2\pi \times 1\,\mathrm{ms}^{-1}$ in Figure 8b with $\Delta_p/\Omega_p = 12$.

An alternative solution is to shorten the cutoff time by reducing r_{n1}, which promises the increase in Δ_p and Ω_p at a fixed ratio, yielding thus a larger effective Rabi frequency. Note, however, that due to realistic restrictions in the experiment, Δ_p and Ω_p cannot be increased at will so our Rydberg anti-blockade strategy is limited to finite atoms in a blockade volume, i.e., not-too-dense atomic ensembles with at most six-body interactions.

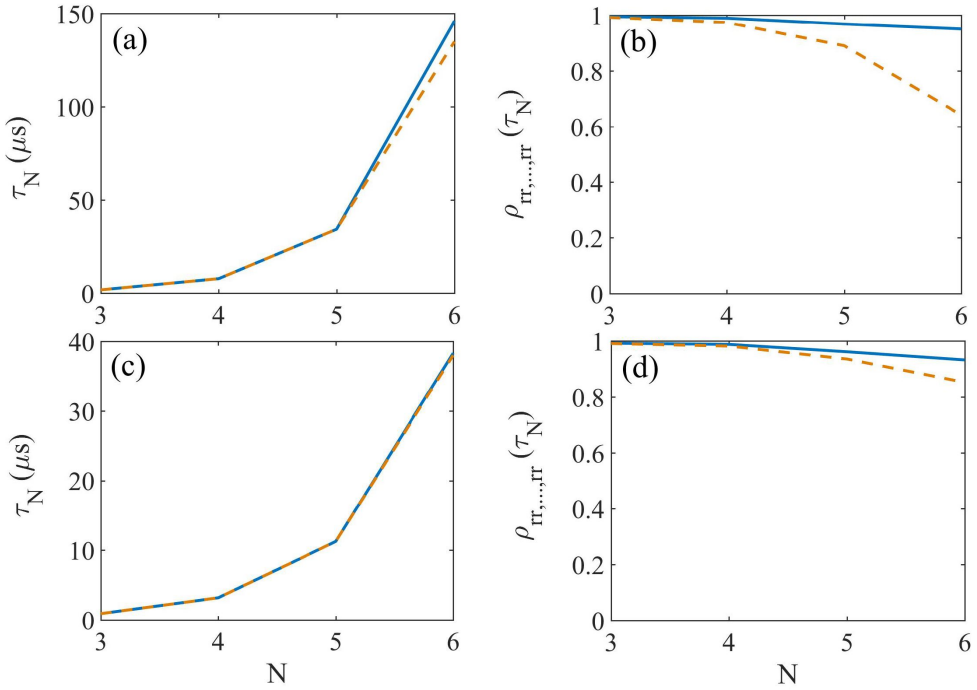

Figure 7. (**a**,**c**) Cutoff time and (**b**,**d**) population of the fully excited state at a corresponding cutoff time against number N of atoms with (**a**,**b**) $\Delta_p/\Omega_p = 15$; (**c**,**d**) $\Delta_p/\Omega_p = 12$. Solid lines refer to $\Gamma = 0$ while dashed lines refer to $\Gamma = 2\pi \times 1\,\mathrm{ms}^{-1}$. Other parameters are the same as in Figure 4.

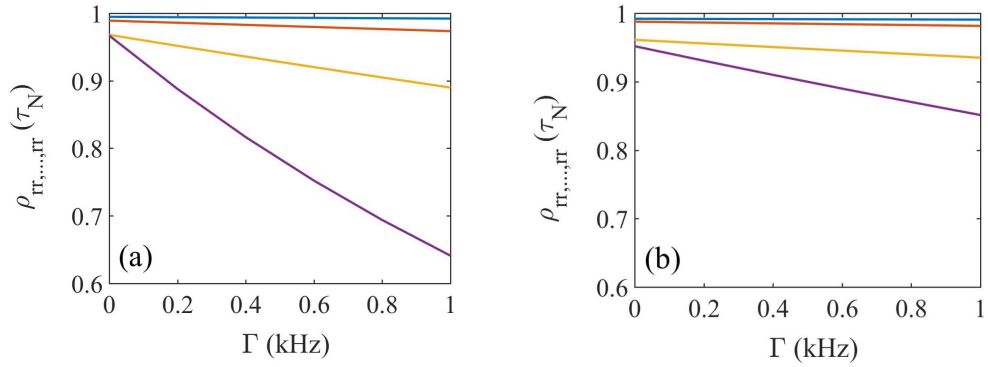

Figure 8. Population of the fully excited state at a corresponding cutoff time against Γ and N with (**a**) $\Delta_p/\Omega_p = 15$; (**b**) $\Delta_p/\Omega_p = 12$. The four lines in each panel correspond to $N = 3$, $N = 4$, $N = 5$, and $N = 6$ in order from top to bottom. Other parameters are the same as in Figure 4.

4. Conclusions

In summary, we have studied the possible realizations of collective anti-blockade excitations for a few Rydberg atoms equally arranged along a ring. By discussing the cases of odd and even numbers of atoms separately, we have derived two general conditions for transferring all atoms from the ground state to the fully excited state yet without populating the intermediate states. We have also derived the effective Rabi frequency answering for population oscillations between the ground and fully excited states, and then the cutoff time of a pump field where all atoms are excited to the Rydberg state. These analytical results have been verified via numerical calculations from which we find that under a certain anti-blockade condition, the collective excitations of all atoms arranged along a ring can be realized at the pump field cutoff time in one step. Note that this cutoff time quickly increases with the number of atoms so that the accumulated effect of spontaneous Rydberg decay becomes more and more significant, which then results in the imperfect Rydberg anti-blockade with the intermediate states being more or less populated. We believe that

our analytical and numerical results exhibit some essential implications for realizing the collective Rydberg anti-blockade; though they do not apply to too many atoms and could be the basis for an experiment leading to a nontrivial quantum light source.

Author Contributions: Conceptualization, Y.F. and J.W.; methodology, Y.F. and J.W.; software, Y.F.; validation, J.W.; formal analysis, Y.F. and J.W.; writing—original draft preparation, Y.F.; writing—review and editing, J.W.; visualization, Y.F.; project administration, J.W. All authors have read and agreed to the published version of the manuscript.

Funding: This research was funded by the National Natural Science Foundation of China (No. 12074061).

Institutional Review Board Statement: Not applicable.

Informed Consent Statement: Not applicable.

Data Availability Statement: Not applicable.

Conflicts of Interest: The authors declare no conflict of interest.

Appendix A. Details on Deriving Anti-Blockade Conditions

When deriving the general anti-blockade conditions in Equations (5) and (8), we have considered some details on the geometric arrangement for an odd or even number of equally spaced atoms along a ring. Taking the odd number of atoms first as an example, in the case of $N = 3$, Equation (3) can be rewritten as

$$\Delta_p = V_1 = \frac{C_6}{r_{n1}^6} \gg \Omega_p, \tag{A1}$$

where $r_{12} = r_{23} = r_{31} = r_{n1}$ is the nearest neighbor interatomic distance as shown in Figure A1a.

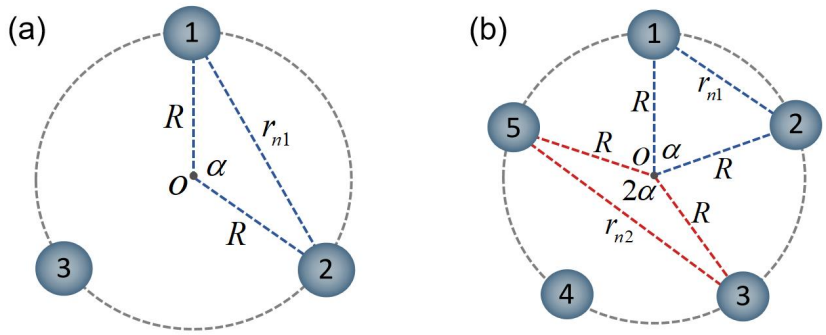

Figure A1. Geometric arrangement of (**a**) three or (**b**) five equally spaced atoms along a ring of center O and radius R. Here, r_{n1} and r_{n2} represent the nearest and the next-nearest neighbor interatomic distances, respectively; $\alpha = 2\pi/N$ with (**a**) $N = 3$ or (**b**) $N = 5$ represents the angle $\angle iO(i+1)$ for $i < N$ or $\angle iO1$ for $i = N$.

In the case of $N = 5$, we know from Figure A1b that Equation (4) instead becomes

$$\Delta_p = V_1 + V_2 = \frac{C_6}{r_{n1}^6} + \frac{C_6}{r_{n2}^6} \gg \Omega_p, \tag{A2}$$

where $r_{12} = r_{23} = r_{34} = r_{45} = r_{51} = r_{n1}$ and $r_{13} = r_{14} = r_{24} = r_{25} = r_{35} = r_{n2}$ are the nearest and the next-nearest neighbor interatomic distances, respectively. Now, we try to express r_{n2} in terms of r_{n1} and the angle $\alpha = 2\pi/5$, as defined in Figure 8b with respect to ring center O and two nearest neighbor atoms. It is easy to learn from the (blue) acute triangle that $r_{n1} = 2R\sin(\alpha/2)$ and from the (red) obtuse triangle that $r_{n2} = 2R\sin(\alpha)$.

Then, we can attain $r_{n2} = r_{n1}\sin(\alpha)/\sin(\alpha/2)$ so that the five-atom anti-blockade condition turns out to be

$$\Delta_p = \frac{C_6}{r_{n1}^6} + \frac{C_6}{\left(r_{n1}\frac{\sin\alpha}{\sin\frac{\alpha}{2}}\right)^6} \gg \Omega_p. \tag{A3}$$

Similarly, in the case of $N = 7$, we can attain

$$\Delta_p = \frac{C_6}{r_{n1}^6} + \frac{C_6}{\left(r_{n1}\frac{\sin\alpha}{\sin\frac{\alpha}{2}}\right)^6} + \frac{C_6}{\left(r_{n1}\frac{\sin\frac{3\alpha}{2}}{\sin\frac{\alpha}{2}}\right)^6} \gg \Omega_p, \tag{A4}$$

which, through a straightforward induction, has been generalized to yield Equation (5).

As an even number of atoms are involved, with the same definitions of α, r_{n1}, r_{n2}, ..., we can attain

$$\Delta_p = \frac{C_6}{r_{n1}^6} + \frac{1}{2}\frac{C_6}{\left(r_{n1}\frac{1}{\sin\frac{\alpha}{2}}\right)^6} \gg \Omega_p, \tag{A5}$$

from Equation (6) in the case of $N = 4$, while

$$\Delta_p = \frac{C_6}{r_{n1}^6} + \frac{C_6}{\left(r_{n1}\frac{\sin\alpha}{\sin\frac{\alpha}{2}}\right)^6} + \frac{1}{2}\frac{C_6}{\left(r_{n1}\frac{1}{\sin\frac{\alpha}{2}}\right)^6} \gg \Omega_p, \tag{A6}$$

from Equation (7) in the case of $N = 6$. They have been generalized to yield Equation (8).

Appendix B. Details on Deriving Effective Hamiltonians

We start by showing some details on deriving the three-atom effective Hamiltonian in Equation (9). The total Hamiltonian of a three-atom system can be rewritten on the three-atom basis as $\mathcal{H}_3 = \mathcal{H}_3^I + \mathcal{H}_3^0$ with

$$\begin{aligned}\mathcal{H}_3^I &= \hbar[\Omega_p(|ggg\rangle\langle ggr| + |ggg\rangle\langle grg| + |ggg\rangle\langle rgg| + |ggr\rangle\langle grr| \\ &+ |ggr\rangle\langle rgr| + |grg\rangle\langle grr| + |grg\rangle\langle rrg| + |rgg\rangle\langle rgr| \\ &+ |rgg\rangle\langle rrg| + |grr\rangle\langle rrr| + |rgr\rangle\langle rrr| + |rrg\rangle\langle rrr|) + H.c.],\end{aligned} \tag{A7}$$

and

$$\begin{aligned}\mathcal{H}_3^0 &= -\hbar\Delta_p(|rgg\rangle\langle rgg| + |grg\rangle\langle grg| + |rgg\rangle\langle rgg|) \\ &+ \hbar(V_1 - 2\Delta_p)(|grr\rangle\langle grr| + |rgr\rangle\langle rgr| + |rrg\rangle\langle rrg|) \\ &+ \hbar(3V_1 - 3\Delta_p)|rrr\rangle\langle rrr|.\end{aligned} \tag{A8}$$

Moving to the rotation frame with respect to $U_3 = e^{i\mathcal{H}_3^0 t/\hbar}$, it is viable to transform $\mathcal{H}_3^I$ into

$$\begin{aligned}\mathcal{H}_3' &= \hbar\Omega_p e^{i\Delta_p t}(|ggg\rangle\langle ggr| + |ggg\rangle\langle grg| + |ggg\rangle\langle rgg|) \\ &+ \hbar\Omega_p e^{i(\Delta_p - 2V_1)t}(|grr\rangle\langle rrr| + |rgr\rangle\langle rrr| + |rrg\rangle\langle rrr|) \\ &+ \hbar\Omega_p e^{i(\Delta_p - V_1)t}(|ggr\rangle\langle grr| + |ggr\rangle\langle rgr| + |grg\rangle\langle grr| \\ &+ |grg\rangle\langle rrg| + |rgg\rangle\langle rgr| + |rgg\rangle\langle rrg|) + H.c.,\end{aligned} \tag{A9}$$

based on which a perturbation method can be used to calculate the effective Hamiltonian $\mathcal{H}_3^{\mathtt{eff}}$.

Under the anti-blockade condition $\Delta_p = V_1 \gg \Omega_p$, we first obtain with

$$\begin{aligned}
& \frac{|ggg\rangle\langle ggg|\mathcal{H}_3'|ggr\rangle\langle ggr|\mathcal{H}_3'|grr\rangle\langle grr|\mathcal{H}_3'|rrr\rangle\langle rrr|}{\Delta_p^2} \\
+ & \frac{|ggg\rangle\langle ggg|\mathcal{H}_3'|ggr\rangle\langle ggr|\mathcal{H}_3'|rgr\rangle\langle rgr|\mathcal{H}_3'|rrr\rangle\langle rrr|}{\Delta_p^2} \\
+ & \frac{|ggg\rangle\langle ggg|\mathcal{H}_3'|grg\rangle\langle grg|\mathcal{H}_3'|grr\rangle\langle grr|\mathcal{H}_3'|rrr\rangle\langle rrr|}{\Delta_p^2} \\
+ & \frac{|ggg\rangle\langle ggg|\mathcal{H}_3'|grg\rangle\langle grg|\mathcal{H}_3'|rrg\rangle\langle rrg|\mathcal{H}_3'|rrr\rangle\langle rrr|}{\Delta_p^2} \\
+ & \frac{|ggg\rangle\langle ggg|\mathcal{H}_3'|rgg\rangle\langle rgg|\mathcal{H}_3'|rgr\rangle\langle rgr|\mathcal{H}_3'|rrr\rangle\langle rrr|}{\Delta_p^2} \\
+ & \frac{|ggg\rangle\langle ggg|\mathcal{H}_3'|rgg\rangle\langle rgg|\mathcal{H}_3'|rrg\rangle\langle rrg|\mathcal{H}_3'|rrr\rangle\langle rrr|}{\Delta_p^2},
\end{aligned} \tag{A10}$$

the effective Rabi frequency $\Omega_3^{\mathtt{eff}} = 6\Omega_p^3/\Delta_p^2$ between states $|ggg\rangle$ and $|rrr\rangle$; second, we obtain with

$$\begin{aligned}
& \frac{|ggg\rangle\langle ggg|\mathcal{H}_3'|ggr\rangle\langle ggr|\mathcal{H}_3'|ggg\rangle\langle ggg|}{\Delta_p} + \frac{|ggg\rangle\langle ggg|\mathcal{H}_3'|grg\rangle\langle grg|\mathcal{H}_3'|ggg\rangle\langle ggg|}{\Delta_p} \\
+ & \frac{|ggg\rangle\langle ggg|\mathcal{H}_3'|rgg\rangle\langle rgg|\mathcal{H}_3'|ggg\rangle\langle ggg|}{\Delta_p},
\end{aligned} \tag{A11}$$

and

$$\begin{aligned}
& \frac{|rrr\rangle\langle rrr|\mathcal{H}_3'|grr\rangle\langle grr|\mathcal{H}_3'|rrr\rangle\langle rrr|}{\Delta_p} + \frac{|rrr\rangle\langle rrr|\mathcal{H}_3'|rgr\rangle\langle rgr|\mathcal{H}_3'|rrr\rangle\langle rrr|}{\Delta_p} \\
+ & \frac{|rrr\rangle\langle rrr|\mathcal{H}_3'|rrg\rangle\langle rrg|\mathcal{H}_3'|rrr\rangle\langle rrr|}{\Delta_p},
\end{aligned} \tag{A12}$$

a common Stark shift $\delta_3^{\mathtt{eff}} = 3\Omega_p^2/\Delta_p$ for states $|ggg\rangle$ and $|rrr\rangle$. Then, we can write down $\mathcal{H}_3^{\mathtt{eff}}$ in Equation (9).

Similarly, we can write down the effective Hamiltonians

$$\begin{aligned}
\mathcal{H}_4^{\mathtt{eff}} &= \left(\frac{4\hbar\Omega_p^2}{\Delta_p}|gggg\rangle\langle gggg| + \frac{4\hbar\Omega_p^2}{\Delta_p}|rrrr\rangle\langle rrrr|\right) \\
&+ \left[\frac{\hbar\Omega_p^4}{\Delta_p^2}\left(\frac{16}{V_1+V_2} + \frac{4}{V_1}\right)|gggg\rangle\langle rrrr| + H.c\right],
\end{aligned} \tag{A13}$$

for a four-atom system under the anti-blockade condition $\Delta_p = V_1 + 0.5V_2 \gg \Omega_p$;

$$\begin{aligned}
\mathcal{H}_5^{\mathtt{eff}} &= \left(\frac{5\hbar\Omega_p^2}{\Delta_p}|ggggg\rangle\langle ggggg| + \frac{5\hbar\Omega_p^2}{\Delta_p}|rrrrr\rangle\langle rrrrr|\right) \\
&+ \left\{\frac{40\hbar\Omega_p^5}{\Delta_p^2}\left[\frac{1}{(V_1+2V_2)^2} + \frac{1}{(V_1+2V_2)(2V_1+V_2)} + \frac{1}{(2V_1+V_2)^2}\right]\right. \\
&\left. |ggggg\rangle\langle rrrrr| + H.c.\right\},
\end{aligned} \tag{A14}$$

for a five-atom system under the anti-blockade condition $\Delta_p = V_1 + V_2 \gg \Omega_p$;

$$\begin{aligned}\mathcal{H}_6^{\mathtt{eff}} &= \left(\frac{6\hbar\Omega_p^2}{\Delta_p}|ggggg\rangle\langle ggggg| + \frac{6\hbar\Omega_p^2}{\Delta_p}|rrrrr\rangle\langle rrrrr|\right) \\ &+ \left\{\frac{\hbar\Omega_p^6}{\Delta_p^2}\left[\frac{96}{(V_1+2V_2+V_3)^2(V_1+2V_2+1.5V_3)}\right.\right. \\ &+ \frac{144}{(V_1+2V_2+V_3)(V_1+2V_2+1.5V_3)(2V_1+V_2+V_3)} \\ &+ \frac{120}{(V_1+2V_2+V_3)(2V_1+2V_2+0.5V_3)(2V_1+V_2+V_3)} \\ &+ \frac{48}{(2V_1+V_2+V_3)^2(2V_1+2V_2+0.5V_3)} \\ &+ \frac{96}{(V_1+2V_2+V_3)(2V_1+2V_2+0.5V_3)(2V_1+2V_2)} \\ &+ \frac{168}{(2V_1+V_2+V_3)(2V_1+2V_2+0.5V_3)(2V_1+2V_2)} \\ &+ \left.\left.\frac{48}{(2V_1+V_2+V_3)(3V_1+1.5V_3)(2V_1+2V_2)}\right]\right. \\ &\left.|ggggg\rangle\langle rrrrr| + H.c.\right\}, \end{aligned} \tag{A15}$$

for a six-atom system under the anti-blockade condition $\Delta_p = V_1 + V_2 + 0.5V_3 \gg \Omega_p$. With these effective Hamiltonians, it is viable to further define effective Rabi frequencies $\Omega_4^{\mathtt{eff}}$, $\Omega_5^{\mathtt{eff}}$, and $\Omega_6^{\mathtt{eff}}$ depending on various Rydberg interactions as well as common Stark shifts $\delta_4^{\mathtt{eff}}$, $\delta_5^{\mathtt{eff}}$, and $\delta_6^{\mathtt{eff}}$ independent of all Rydberg interactions.

References

1. Saffman, M.; Walker, T.G.; Mølmer, K. Quantum information with Rydberg atoms. *Rev. Mod. Phys.* **2010**, *82*, 2313–2363. [CrossRef]
2. Sibalic, N. *Rydberg Physics*; IOP Publishing: Bristol, UK, 2018.
3. Vogt, T.; Viteau, M.; Chotia, A.; Zhao, J.; Comparat, D.; Pillet, P. Electric-field induced dipole blockade with Rydberg atoms. *Phys. Rev. Lett.* **2007**, *99*, 073002. [CrossRef] [PubMed]
4. Lukin, M.D.; Fleischhauer, M.; Cote, R.; Duan, L.M.; Jaksch, D.; Cirac, J.I.; Zoller, P. Dipole blockade and quantum information processing in mesoscopic atomic ensembles. *Phys. Rev. Lett.* **2001**, *87*, *037901*. [CrossRef] [PubMed]
5. Yu, D.; Wang, H.; Liu, J.M.; Su, S.L.; Qian, J.; Zhang, W.P. Multiqubit Toffoli gates and optimal geometry with Rydberg atoms. *Phys. Rev. Lett.* **2022**, *18*, 034072. [CrossRef]
6. McDonnell, K.; Keary, L.F.; Pritchard, J.D. Demonstration of a quantum gate using electromagnetically induced transparency. *Phys. Rev. Lett.* **2022**, *129*, 200501. [CrossRef]
7. Zheng, D.D.; Zhang, Y.; Liu, Y.M.; Zhang, X.J.; Wu, J.H. Spatial Kramers-Kronig relation and unidirectional light reflection induced by Rydberg interactions. *Phys. Rev. A* **2023**, *107*, 013704. [CrossRef]
8. Wang, K.W.; Jin, H.; Lei, Y.B.; Zhao, Y.; Huang, K.Y.; Xu, S.L. Two-dimensional solitons in Bose–Einstein condensates with spin–orbit coupling and Rydberg–Rydberg interaction. *Photonics* **2022**, *9*, 283. [CrossRef]
9. Ma, D.; Yu, D.; Zhao, X.-D.; Qian, J. Unidirectional and controllable higher-order diffraction by a Rydberg electromagnetically induced grating. *Phys. Rev. A* **2019**, *99*, 033826. [CrossRef]
10. Young, J.T.; Bienias, P.; Belyansky, R.; Kaufman, A.M.; Gorshkov, A.V. Asymmetric blockade and multiqubit gates via dipole-dipole interactions. *Phys. Rev. Lett.* **2021**, *127*, 120501. [CrossRef]
11. Shi, X.F. Quantum logic and entanglement by neutral Rydberg atoms: Methods and fidelity. *Quantum Sci. Technol.* **2022**, *7*, 023002. [CrossRef]
12. Bai, W.J.; Yan, D.; Han, H.Y.; Hua, S.; Gu, K.H. Correlated dynamics of three-body Rydberg superatoms. *Acta Phys. Sin.* **2022**, *71*, 014202. [CrossRef]
13. Heller, L.; Lowinski, J.; Theophilo, K.; Padron-Brito, A.; de Riedmatten, H. Raman storage of quasideterministic single photons generated by Rydberg collective excitations in a low-noise quantum memory. *Phys. Rev. A* **2022**, *18*, 024036. [CrossRef]
14. Ripka, F.; Kubler, H.; Low, R.; Pfau, T. A room-temperature single-photon source based on strongly interacting Rydberg atoms. *Science* **2020**, *367*, 4382. [CrossRef] [PubMed]

15. Bounds, A.D.; Jackson, N.C.; Hanley, R.K.; Bridge, E.M.; Huillery, P.; Jones, M.P.A. Coulomb anti-blockade in a Rydberg gas. *New J. Phys.* **2019**, *21*, 053026. [CrossRef]
16. Ates, C.; Pohl, T.; Pattard, T.; Rost, J.M. Antiblockade in Rydberg excitation of an ultracold lattice gas. *Phys. Rev. Lett.* **2007**, *98*, 023002. [CrossRef]
17. Amthor, T.; Giese, C.; Hofmann, C.S. Evidence of antiblockade in an ultracold Rydberg gas. *Phys. Rev. Lett.* **2010**, *104*, 013001. [CrossRef]
18. Zuo, Z.; Nakagawa, K. Multiparticle entanglement in a one-dimensional optical lattice using Rydberg-atom interactions. *Phys. Rev. A* **2010**, *82*, 062328. [CrossRef]
19. Lee, T.E.; Häffner, H.; Cross, M.C. Collective quantum jumps of Rydberg atoms. *Phys. Rev. Lett.* **2012**, *108*, 023602. [CrossRef]
20. Su, S.L.; Gao, Y.; Liang, E.; Zhang, S. Fast Rydberg antiblockade regime and its applications in quantum logic gates. *Phys. Rev. A* **2017**, *95*, 022319. [CrossRef]
21. Zheng, R.H.; Xiao, Y.; Su, S.L.; Chen, Y.H.; Shi, Z.C.; Song, J.; Xia, Y.; Zheng, S.B. Fast and dephasing-tolerant preparation of steady Knill-Laflamme-Milburn states via dissipative Rydberg pumping. *Phys. Rev. A* **2021**, *103*, 052402. [CrossRef]
22. Su, S.L.; Liang, E.; Zhang, S.; Wen, J.J.; Sun, L.L.; Jin, Z.; Zhu, A.D. One-step implementation of the Rydberg-Rydberg-interaction gate. *Phys. Rev. A* **2016**, *93*, 012306. [CrossRef]
23. Fan, C.H.; Zhang, H.X.; Wu, J.H. In-phase and antiphase dynamics of Rydberg atoms with distinguishable resonances. *Phys. Rev. A* **2019**, *99*, 033813. [CrossRef]
24. Yan, D.; Bai, W.J.; Bai, J.N.; Chen, L.; Han, H.Y.; Wu, J.H. Dynamical collective excitations and entanglement of two strongly correlated Rydberg superatoms. *Photonics* **2022**, *9*, 242. [CrossRef]
25. Su, S.L.; Tian, Y.; Shen, H.Z.; Zang, H.; Liang, E.; Zhang, S. Applications of the modified Rydberg antiblockade regime with simultaneous driving. *Phys. Rev. A* **2017**, *96*, 042335. [CrossRef]
26. Jandura, S.; Pupillo, G. Time-optimal two- and three-qubit gates for Rydberg atoms. *Quantum* **2022**, *6*, 712. [CrossRef]
27. Su, S.L.; Li, W. Dipole-dipole-interaction-driven antiblockade of two Rydberg atoms. *Phys. Rev. A* **2021**, *104*, 033716. [CrossRef]
28. Chen, X.; Xie, H.; Lin, G.W.; Shang, X.; Ye, M.Y.; Lin, X.M. Dissipative generation of a steady three-atom singlet state based on Rydberg pumping. *Phys. Rev. A* **2017**, *96*, 042308. [CrossRef]
29. Shao, X.Q.; Wu, J.H.; Yi, X.X. Dissipation-based entanglement via quantum Zeno dynamics and Rydberg antiblockade. *Phys. Rev. A* **2017**, *95*, 062339. [CrossRef]
30. Jiao, Y.C.; Hao, L.P.; Fan, J.B.; Bai, J.X.; Zhao, J.M.; Jia, S.T. Autoionization of ultracold Cesium Rydberg atom in 37D5/2 state. *Photonics* **2022**, *9*, 352. [CrossRef]
31. Jin, Z.; Li, R.; Gong, W.J.; Qi, Y.; Zhang, S.; Su, S.L. Implementation of the Rydberg double anti-blockade regime and the quantum logic gate based on resonant dipole-dipole interactions. *Acta Phys. Sin.* **2010**, *70*, 134202. [CrossRef]
32. Endres, M.; Bernien, H.; Keesling, A.; Levine, H.; Anschuetz, E.R.; Krajenbrink, A.; Senko, C.; Vuletic, V.; Greiner, M.; Lukin, M.D. Atom-by-atom assembly of defect-free one-dimensional cold atom arrays. *Science* **2016**, *354*, 1024–1027. [CrossRef] [PubMed]
33. Barredo, D.; de Léséleuc, S.; Lienhard, V.; Lahaye, T.; Browaeys, A. An atom-by-atom assembler of defect-free arbitrary two-dimensional atomic arrays. *Science* **2016**, *354*, 1021–1023. [CrossRef]
34. Yu, S.; He, X.; Xu, P.; Liu, M.; Wang, J.; Zhan, M. Single atoms in the ring lattice for quantum information processing and quantum simulation. *Chin. Sci. Bull.* **2012**, *57*, 1931–1945. [CrossRef]
35. Barredo, D.; Lienhard, V.; de Léséleuc, S.; Lahaye, T.; Browaeys, A. Synthetic three-dimensional atomic structures assembled atom by atom. *Nature* **2018**, *561*, 79–82. [CrossRef] [PubMed]
36. Sheng, C.; Hou, J.; He, X.; Wang, K.; Guo, R.; Zhuang, J.; Mamat, B.; Xu, P.; Liu, M.; Wang, J.; et al. Defect-free arbitrary-geometry assembly of mixed-species atom arrays. *Phys. Rev. Lett.* **2022**, *128*, 083202. [CrossRef]
37. Wu, H.; Huang, X.R.; Hu, C.S.; Yang, Z.B.; Zheng, S.B. Rydberg-interaction gates via adiabatic passage and phase control of driving fields. *Phys. Rev. A* **2017**, *96*, 022321. [CrossRef]
38. Petrosyan, D.; Motzoi, F.; Saffman, M.; Mølmer, K. High-fidelity Rydberg quantum gate via a two-atom dark state. *Phys. Rev. A* **2017**, *96*, 042306. [CrossRef]
39. Zeng, Y.; Xu, P.; He, X.; Liu, Y.; Liu, M.; Wang, J.; Papoular, D.J.; Shlyapnikov, G.V.; Zhan, M. Entangling two individual atoms of different isotopes via Rydberg blockade. *Phys. Rev. Lett.* **2017**, *119*, 160502. [CrossRef]
40. Beterov, I.I.; Ashkarin, I.N.; Yakshina, E.A.; Tretyakov, D.B.; Entin, V.M.; Ryabtsev, I.I.; Cheinet, P.; Pillet, P.; Saffman, M. Fast three-qubit Toffoli quantum gate based on three-body Förster resonances in Rydberg atoms. *Phys. Rev. A* **2018**, *98*, 042704. [CrossRef]
41. Shi, X.F. Deutsch, Toffoli, and CNOT gates via Rydberg blockade of neutral atoms. *Phys. Rev. A* **2018**, *9*, 051001. [CrossRef]
42. Labuhn, H.; Barredo, D.; Ravets, S.; de Léséleuc, S.; Macrì, T.; Lahaye, T.; Browaeys, A. Tunable two-dimensional arrays of single Rydberg atoms for realizing quantum Ising models. *Nature* **2016**, *534*, 667–670. [CrossRef] [PubMed]
43. Bernien, H.; Schwartz, S.; Keesling, A.; Levine, H.; Omran, A.; Pichler, H.; Choi, S.; Zibrov, A.S.; Endres, M.; Greiner, M.; et al. Probing many-body dynamics on a 51-atom quantum simulator. *Nature* **2017**, *551*, 579–584. [CrossRef] [PubMed]
44. Kim, H.; Park, Y.; Kim, K.; Sim, H.S.; Ahn, J. Detailed balance of thermalization dynamics in Rydberg-atom quantum simulators. *Phys. Rev. Lett.* **2018**, *120*, 180502. [CrossRef] [PubMed]
45. Barredo, D.; Labuhn, H.; Ravets, S.; Lahaye, T.; Browaeys, A.; Adams, C.S. Coherent excitation transfer in a spin chain of three Rydberg atoms. *Phys. Rev. Lett.* **2015**, *114*, 113002. [CrossRef] [PubMed]

46. de Léséleuc, S.; Lienhard, V.; Scholl, P.; Barredo, D.; Weber, S.; Lang, N.; Büchler, H.P.; Lahaye, T.; Browaeys, A. Observation of a symmetry-protected topological phase of interacting bosons with Rydberg atoms. *Science* **2019**, *365*, 775–780. [CrossRef]
47. Olmos, B.; González-Férez, R.; Lesanovsky, I. Creating collective many-body states with highly excited atoms. *Phys. Rev. A* **2010**, *81*, 023604. [CrossRef]
48. Ebadi, S.; Wang, T.T.; Levine, H.; Keesling, A.; Semeghini, G.; Omran, A.; Bluvstein, D.; Samajdar, R.; Pichler, H.; Ho, W.W.; et al. Quantum phases of matter on a 256-atom programmable quantum simulator. *Nature* **2021**, *595*, 227–232. [CrossRef]
49. Scholl, P.; Schuler, M.; Williams, H.J.; Eberharter, A.A.; Barredo, D.; Schymik, K.N.; Lienhard, V.; Henry, L.P.; Lang, T.C.; Lahaye, T.; et al. Quantum simulation of 2D antiferromagnets with hundreds of Rydberg atoms. *Nature* **2021**, *595*, 233–238. [CrossRef]
50. Šibalić, N.; Pritchard, J.D.; Adams, C.S.; Weatherill, K.J. An Introduction to Rydberg Atoms with ARC. Available online: https://arc-alkali-rydberg-calculator.readthedocs.io/en (accessed on 23 April 2023).
51. Yang, H.; Yang, L.; Wang, X.C.; Cui, C.L.; Zhang, Y.; Wu, J.H. Dynamically controlled two-color photonic band gaps via balanced four-wave mixing in one-dimensional cold atomic lattices. *Phys. Rev. A* **2013**, *88*, 063832. [CrossRef]
52. Schilke, A.; Zimmermann, C.; Courteille, P.W.; Guerin, W. Photonic band gaps in one-dimensionally ordered cold atomic vapors. *Phys. Rev. Lett.* **2011**, *106*, 223903. [CrossRef]
53. Schilke, A.; Zimmermann, C.; Guerin, W. Photonic properties of one-dimensionally-ordered cold atomic vapors under conditions of electromagnetically induced transparency. *Phys. Rev. A* **2012**, *86*, 023809. [CrossRef]
54. James, D.F.; Jerke, J. Effective Hamiltonian theory and its applications in quantum information. *Can. J. Phys.* **2007**, *85*, 625–632. [CrossRef]
55. Beterov, I.I.; Ryabtsev, I.I.; Tretyakov, D.B.; Entin, V.M. Erratum: Quasiclassical calculations of blackbody-radiation-induced depopulation rates and effective lifetimes of Rydberg nS, nP, and nDalkali-metal atoms with ≤ 80. *Phys. Rev. A* **2009**, *79*, 052504. [CrossRef]